

Journal of Rehabilitation in Civil Engineering

Journal homepage: <https://civiljournal.semnan.ac.ir/>

## Prediction of Impact Response for Reinforced Concrete Beams by Numerical Simulation Method

Ahmad Rahmati Alaei <sup>1,\*</sup> ; Seyed Mohammad Hosein Khatami <sup>2</sup>

1. Assistant Professor, Department of Mechanical Engineering, National University of Skills (NUS), Tehran, Iran

2. Department of Civil Engineering, National University of Skills (NUS), Tehran, Iran

\* Corresponding author: [arahmatialaei@tvu.ac.ir](mailto:arahmatialaei@tvu.ac.ir)

### ARTICLE INFO

#### Article history:

Received: 02 July 2024

Revised: 11 August 2024

Accepted: 30 October 2024

#### Keywords:

Reinforced concrete;

Finite element;

Impact response;

Bending failure;

Drop hammer test.

### ABSTRACT

Brittle characteristics, low tensile strength, and rapid crack propagation upon exposure to impact loads are some of the issues associated with concrete. This study predicts reinforced concrete (RC) beam failure modes under impact loads using experimental tests and numerical simulations. This paper simulates the drop test of a hammer using the nonlinear finite element method (FEM) and the powerful FE analysis software LS-DYNA. The developed model, unlike other numerical research, boasts a high computational speed and can effectively simulate real impact test conditions, like a vehicle collision with a bridge barrier. Also, the material models introduced for concrete and steel can be used in low to high strain rates for impact with different loading rates (LR). The components of the model include concrete, rebar, stirrup, and hammer. The reinforcement is modeled by beam elements, while the other parts consist of solid elements with an average size of 10mm. CONCRETE DAMAGE and PEICEWISE LINEAR PLASTICITY are used for describing the material behavior of concrete and rebar-stirrup, respectively. The interaction between parts, due to the different behavior of their materials, is carefully considered in the analysis. The difference in maximum displacement at beam midpoint between the impact test and the numerical simulation is less than 8%, highlighting an acceptable agreement between the results. The plastic strain contour for the RC sample test S1616 shows flexural failure modes at a drop height of 0.15 meters. The effects of the loading rate (LR) and concrete compressive strength are discussed. For every 10 MPa improvement in concrete compressive strength, mid span displacement decreased by about 10%. Impact force increases by roughly 31% at high loading rates (LR = 10 m/s), and compressive strength ranges from 32 MPa to 52 MPa.

E-ISSN: 2345-4423

© 2025 The Authors. Journal of Rehabilitation in Civil Engineering published by Semnan University Press.

This is an open access article under the CC-BY 4.0 license. (<https://creativecommons.org/licenses/by/4.0/>)

#### How to cite this article:

Rahmati Alaei, A., & Khatami, S. M. H. (2025). Prediction of Impact Response for Reinforced Concrete Beams by Numerical Simulation Method. Journal of Rehabilitation in Civil Engineering, 13(2), 182-197. <https://doi.org/10.22075/jrce.2024.34616.2128>

## **1. Introduction**

Designs for reinforced concrete (RC) constructions should be for low-speed impact loads due to their exposure to falling rocks in mountainous areas, as well as heavy loads falling in factories and warehouses. The main weaknesses of concrete include brittle behavior, low tensile strength, and rapid expansion of cracks, so that when exposed to dynamic loads such as impact, in addition to its damage, it may damage the surrounding environment due to spalling [1–3]. So, in recent years, evaluating the performance and reducing the vulnerability of RC structures under the influence of impact loads has become an important issue for engineers and designers.

Impact loading is a very intense loading mode that is applied in a very short time. In impact loading, the behavior of materials is different in the fracture zone pattern and impact energy consumption mechanism. Brittle materials typically consume elastic energies as surface energy without forming a failure area. Plastic failure areas in ductile materials can consume a lot of energy. For semi brittle materials, a large failure area that consumes a large amount of energy before failure is usually formed.

So far, a lot of research has been done regarding the effect of impact on concrete. ACI 544 [4] has proposed the weight drop test to evaluate the impact resistance of concrete. This test is widely used due to its simplicity and low cost, but the data obtained from it often has a large dispersion [5] and coefficient of variation greater than 25%. In the Reddy study [6,7], the behavior of HSC slabs was compared to entrenched reinforced slabs in the same arrangement. When strengthening investigated, dynamic measures including maximum acceleration and index of structural damage—the energy needed to generate a unit fracture length from an impact—were found to be dependent on steel ratio.

In order to accurately assess the safety of RC beams subjected to impact loading, the estimation of the bending capacity and the response of their maximum deformation is considered an important index of failure [7–11]. On the other hand, providing a reliable model based on numerical methods such as finite element (FE), boundary element (BE), etc., which has the ability to examine the impact load behavior of RC structures, has always been considered by researchers by extracting parameters and relationships affecting cracking. They have proposed factors to prevent and reduce damage to these structures [12–14].

Utilizing both experimental and numerical methods, Anil et. al. [15] examined the behaviors of RC beams in ECC concrete with PVA fibers, as well as in low- and normal-strength concrete. Ozbolt et al. [16] created a numerical simulation of RC beams under impact for failure patterns and the effect of shear reinforcements. They discovered that the loading rate has a significant effects on the failure mechanism of RC beams. Several numerical investigations employing FE code are conducted for impact assessments of RC beams.

The load-carrying capacity of RC beam column joints was calculated using soft computing approaches, such as multilinear regression with a genetic algorithm and an artificial neural network (ANN) [17–19]. The experimental and numerical analyses are performed on the strength of concrete beams reinforced with steel bars and Fiber-Reinforced Polymer (FRP) under impact [20,21]. Recently, wavelet transform-based numerical models have been suggested to assess damages and crack propagation trends in reinforced concrete beams of different severities and locations [22,23].

This paper uses the powerful FE analysis software LS-DYNA to simulate the drop hammer test on a RC beam based on Fujikake et al.'s experimental test [14]. The numerical model presented in this study can be a practical tool to predict the failure modes of RC beams under different loadings and

reduce the costs of destructive tests. This FE code performs numerical calculations quickly in 3D analysis compared to other numerical research. The material model of the RC beam in this study can represent concrete's complex behavior in compression and tension at different strain rates and predict the crack pattern. The suggested FE model enables parametric impact loading assessments, such as bridge structure under vehicle collisions. The agreement of the results obtained in the numerical analysis with the experimental test confirms the validity of the numerical model in this paper.

In the nonlinear analysis to evaluate the bending capacity of RC beams, the effect of the vertical distance from which an object falls and the quantity of reinforcement placed along the length of a structure are considered. The fracture index of RC beams is based on the maximum mid span deformation of the RC beam and the maximum impact load. After the validation of the numerical result, the mesh convergence study for RC beam deflection and impact force is performed for the independence of the results from the element size. The loading rate and compressive strength of concrete were the variables examined in the parametric investigation. The bending failure mode of RC beams with low 32 MPa, medium 42 MPa, and high 52 MPa compressive strength are compared at LR= 2, 4, 6, 8, and 10 m/s.

## 2. Experimental test description

### 2.1. Impact response of concrete

The behavior of concrete beam under impact loading includes two phases of response, according to Fig. 1. The stress wave at the loading point, which occurs very quickly after the impact, causes the local response, and the elastic-plastic deformation, which occurs over a long period of time in the entire concrete structure, causes the overall response. The overall response is mostly determined by the loading rate effect and the structure's dynamic behavior.

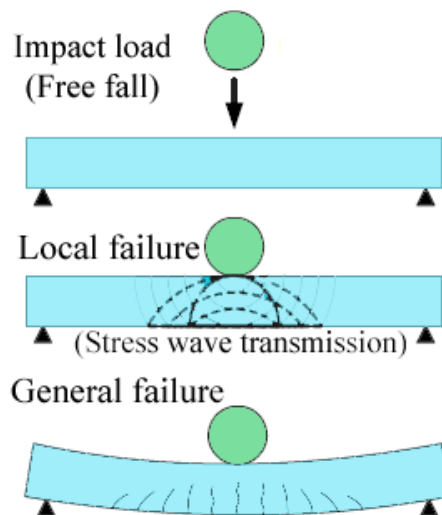


Fig. 1. Impact response of RC.

### 2.2. Drop hammer test of rc beam

As shown in Fig. 2, the dimensions of the drop impact test [24] are 1700 mm in length and 150 mm x 250 mm in cross-sectional area. According to Table 1, the longitudinal reinforcement includes D16 with a yield stress of 426 MPa. D10 bars with a distance of 75 mm and yield stress of 295 MPa have been used as stirrups.

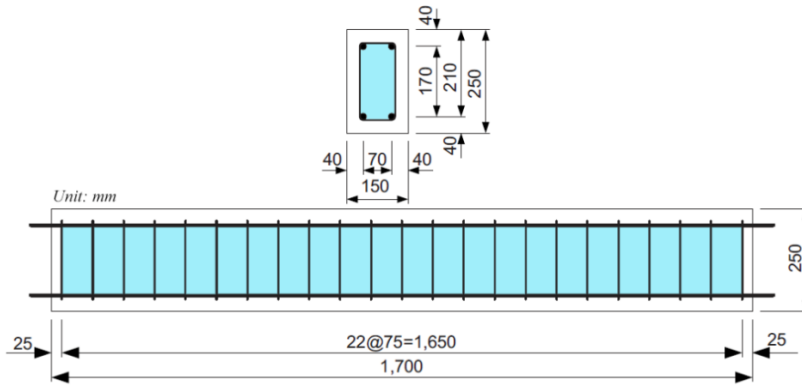


Fig. 2. Dimensions of RC beam with steel bar.

In accordance with the JSCE concrete standard [24], the RC beam's bending and shear strengths are computed, and specified in Table 2.

Table 1. Rebar arrangement in concrete.

Sample	Compression state		Tension state	
	Number-Size (mm)	$A_s$ (mm <sup>2</sup> )	Number-Size (mm)	(mm <sup>2</sup> ) $A_s$
S1616	2_D16	397	2_D16	397

Table 3 shows the concrete mix fraction in this test. Concrete has compressive strength equivalent to 42 MPa, and the employed aggregates have a maximum size of 10 mm.

Table 2. Bending and shear strength of rebars.

Sample	Bending strength	Shear strength	RS /RM
	RM	RS	
S1616	91.1	232	2.55

For applying impact loading, according to Fig. 3.a drop hammer setup was used. A 400-kg hammer is dropped from the upper surface and in the middle span of the RC beam by a height of 0.15 m. RC beam support along a 1400 mm span with its special design allows for free rotation; while the displacement degree of freedom is fixed. Hammer-RC contact force and the middle deformation of the concrete beam are measured using a dynamic force sensor (load cell) and a laser displacement sensor, respectively (Fig. 3). A thin plastic sheet is installed on the bottom surface of the RC, which increases the accuracy of the laser sensor to record the response by 100 kHz sampling.

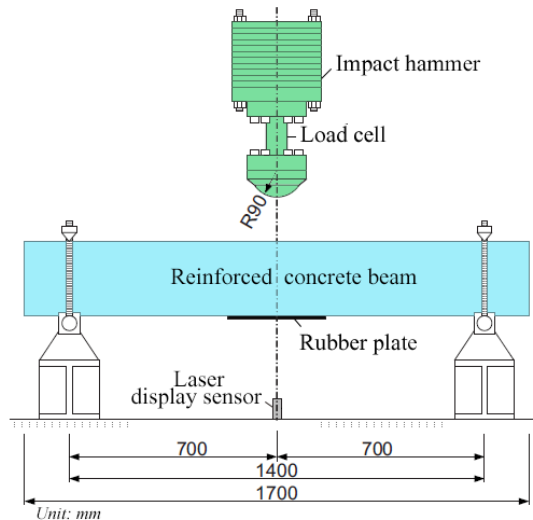


Fig. 3. Details of the experimental setup.

### 3. Finite element method simulation

In this paper, the powerful finite element (FE) analysis software LS-DYNA is used to simulate the hammer drop impact on RC with the explicit dynamic nonlinear finite element method (FEM). This software describes material behavior using roughly 190 material behavior models and 13 equations of state (EOS).

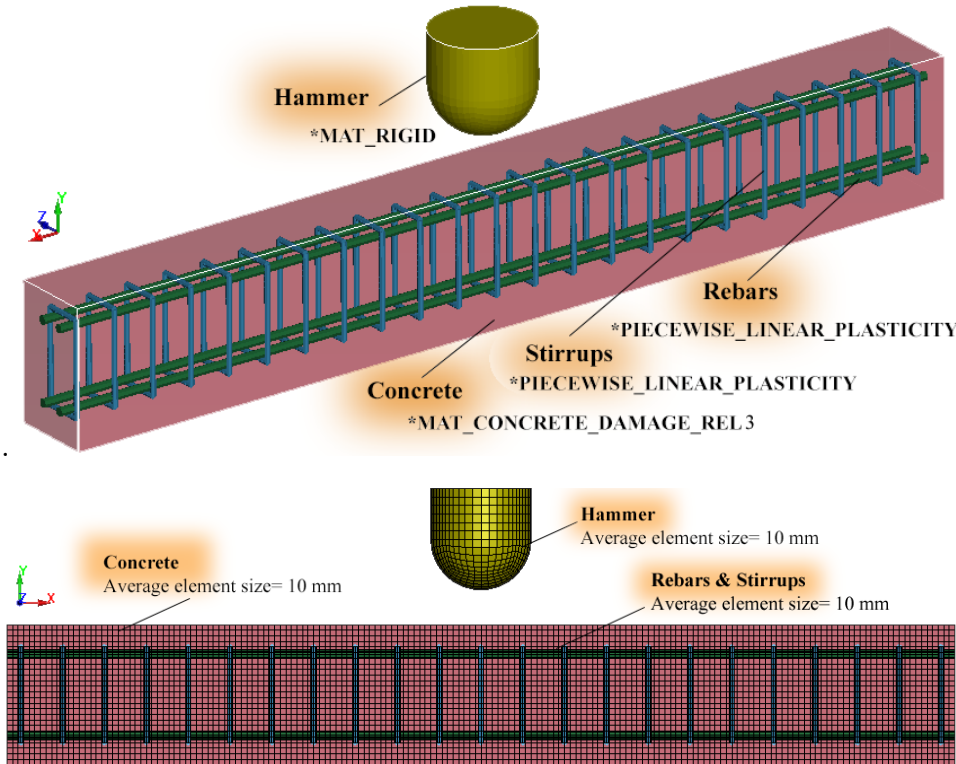


Fig. 4. Finite element model for drop hammer impact on RC.

By applying the correct conditions of the physics of the problem, including the material model, boundary conditions, contact algorithms, loadings, and good element quality for meshing, it is possible to extract results with high accuracy in comparison with experimental tests. The numerical model is developed according to Fujikake et al.'s [25] with the dimensions of Fig. 3, in LS-DYNA is shown in Fig. 4. The material model of concrete includes the definition of the stress-strain relationship, the failure criterion, and post-cracking behavior. LS-DYNA software has several material models to describe concrete behavior.

#### 3.1. Constitutive material models

MAT\_CONCRETE\_DAMAGE material model is capable of modeling the complex behavior of concrete in compression and tension under loads, even with a high strain rate [26].

Table 3. Mix proportion of concrete [25].

Unit weight (kg/m <sup>3</sup> )					Air(%)	Slump (cm)
W	C	S	G	Ad		
185	416	726	943	4.16	4.5	15.5

G=gravel, S=sand, C=cement, W=water. Ad=addition.

The theory of concrete fracture in this material model is based on Malvar's [27] and the fracture surface of concrete is defined according to the Willam-Warnke [28] as follows:

Maximum failure level:

$$\Delta\sigma_m = a_0 + \frac{p}{a_1+a_2p} \tag{1}$$

Residual failure level:

$$\Delta\sigma_r = a_0 + \frac{p}{a_{1f}+a_{2f}p} \tag{2}$$

Yeild failure level:

$$\Delta\sigma_y = a_{0y} + \frac{p}{a_{1y}+a_{2y}p} \tag{3}$$

Advanced failure level:

$$\Delta\sigma_e = r_f \nabla \sigma \left( \frac{p}{r_f} \right) \tag{4}$$

The parameters  $a_0$ ,  $a_1$  and  $a_2$  are constants obtained from triaxial compression tests and unconfined compression tests. The enhancement factor for concrete strength  $r_f$  is obtained from Fig. 5. Multiplying this coefficient by concrete's static compressive strength gives the improved strength at each strain rate.

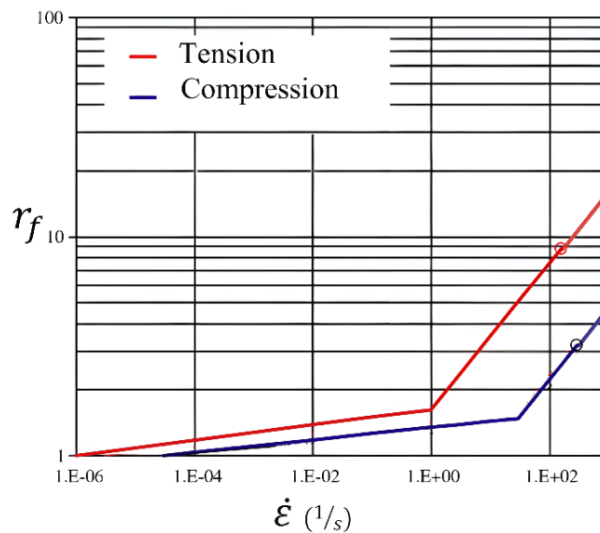


**Fig. 5.** The enhancement factor for concrete strength per strain rate.

MAT\_PEICEWISE\_LINEAR\_PLASTICITY material model is used for steel behavior. This material model in LS-DYNA software is an elastoplastic material model with the ability to define the plastic part in stress-strain curve. In this material model, there is also the ability to define the strain rate effect. The criterion for eroding elements in this material model is plastic strain, or the minimum time step. If the elements reach the failure strain or the time step of the solver is smaller than the specific amount determined in the material model, the software will remove those elements from the calculations. According to Fig. 6, in this model, the stress-strain curve is defined depending on the strain rate.

To model the dynamic behavior of steel rebars, the parameters of increasing resistance are considered. The yield stress function of steel rebar based on Von Mises theory is as follows:

$$\sigma_y = \beta [\sigma_0 + f_h(\epsilon_{eff}^p)] \tag{5}$$

$$\beta = 1 + (\dot{\epsilon}/c)^{1/r} \tag{6}$$

$$f_h(\epsilon_{eff}^p) = E_p(\epsilon_{eff}^p) \tag{7}$$

Since the material of the hammer is very hard steel and does not change its shape, the rigid material model has been chosen for it. Meshing is of special importance in explicit analysis. The length of the element should be strictly controlled, and a regular grid should be used.

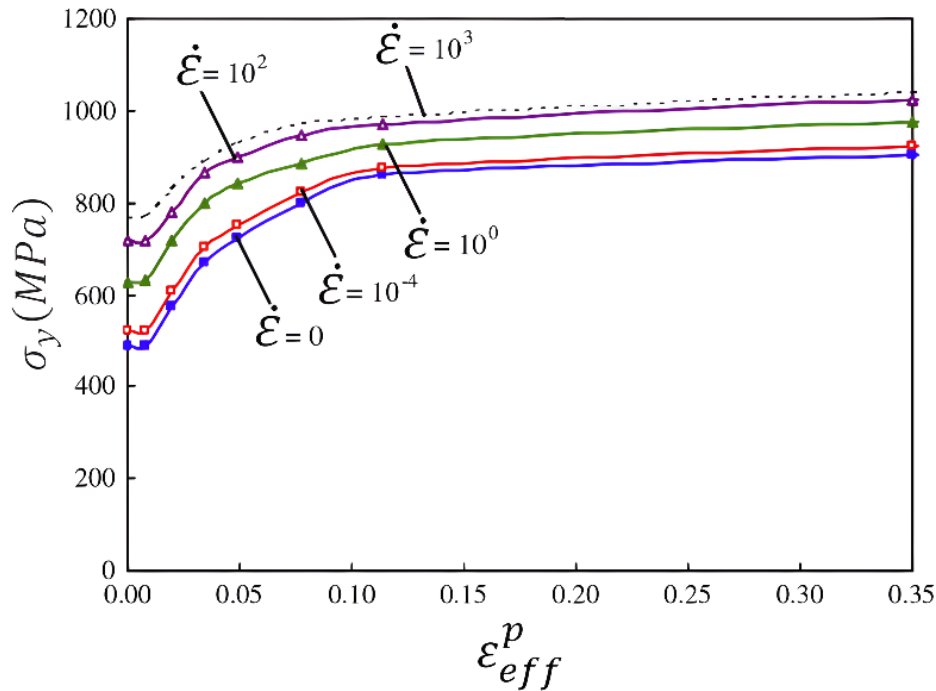


Fig. 6. Strain rate effect on the effective plastic strain of steel [29].

According to Fig. 4 three-dimensional solid elements with an average size of 10 mm are used to model the hammer (impactor) and concrete; this type of element has an 8-node cubic geometry and each node has 9 degrees of freedom, including displacement, velocity and acceleration. The beam element is also selected for modeling the rebars and stirrup. The components of the FE model, including the physical properties of the material model and the type and number of elements, are specified in Table 4.

Table 4. Finite element model components.

	Concrete	Rebar & Stirrup (Reinforcements)	Hammer (Impactor)
Material model	*CONCRETE_DAMAGE_REL3	*PIECEWISE_LINEAR_PLASTICITY	*RIGID
Material parameters	$\rho = 0.0024 \text{ gr/cm}^3$ $S_c = 42 \text{ Mpa}$	$\rho = 0.00783 \text{ gr/cm}^3$ $E = 2e5 \text{ Mpa}$ $\nu = 0.3$ $\sigma_y = 295 \text{ \& } 426 \text{ Mpa}$ $E_t = 689 \text{ Mpa}$	$\rho = 0.15 \text{ gr/cm}^3$ $E = 2.07e5 \text{ Mpa}$ $\nu = 0.3$
Element type	Solid (Hex:CST)	Beam (Hughes-Liu)	Solid (Hex:CST)
Number of elements	63750	680 -1104	10368

The parameters  $\rho$ ,  $\nu$ ,  $\sigma_y$ ,  $E$ ,  $E_t$  and  $S_c$  are density, poisson's ratio, yield stress, elastic modulus, tangent modulus and compressive strength of concrete, respectively.

### 3.2. Contacts & interactions

The contact algorithm is used to express the concept of interaction between different components in numerical simulation. In this study, AUTOMATIC\_SURFACE\_TO\_SURFACE contact model was used for modelling the interaction between RC and hammer. The interaction between reinforcement and concrete, due to the different behavior of steel and concrete, should be carefully considered in FE analysis [30,31]. The inconsistency in the different behavior of steel and concrete due to the higher elastic modulus of steel compared to concrete and also the difference in the behavior of concrete in tension and compression leads to the separation of the contact between steel and concrete, and the result is slippage of reinforcements, local deformations and cracking. For this purpose, in this paper, \*CONSTRAINED\_LAGRANGE\_IN\_SOLID is issued.

## 4. Result and discussion

### 4.1. Validation of numerical model

The common failure mode observed in the drop impact test is illustrated in Fig. 7 for 1616S sample. The beams show general bending failure at the fall height of 0.15 m. Local failure along with concrete crushing is observed in close proximity to the loading area, with a drop distance of under 1.2 meters.

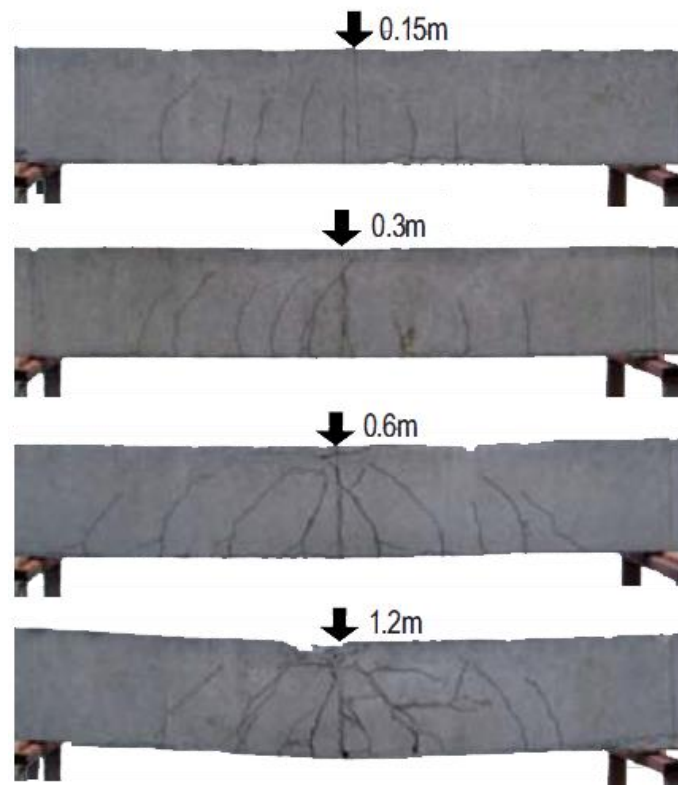


**Fig. 7.** Failure modes of S1616 sample [25].

In the following section, we present a comparison between the drop hammer test and two major characteristics of the finite element method (FEM) to verify numerical simulation results.

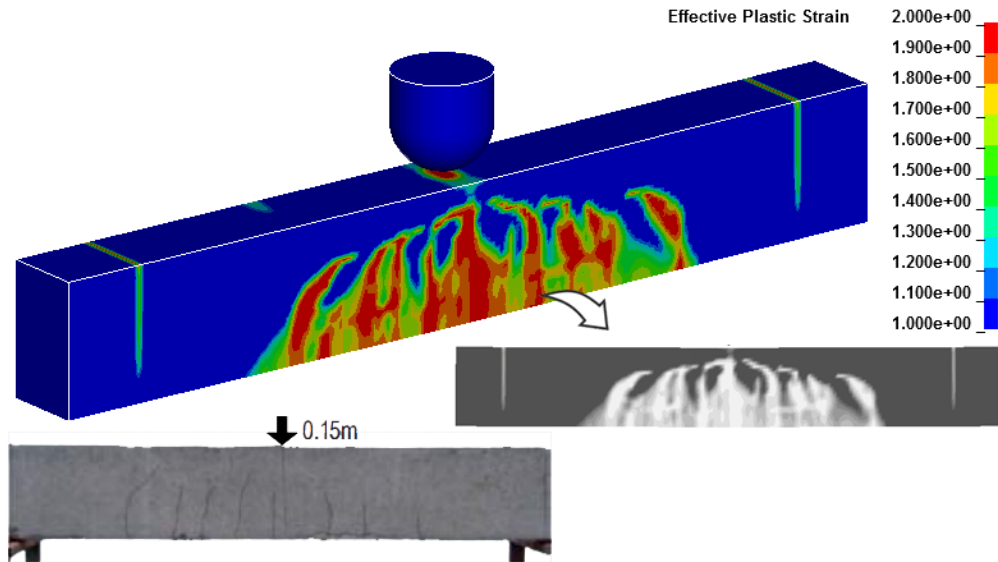
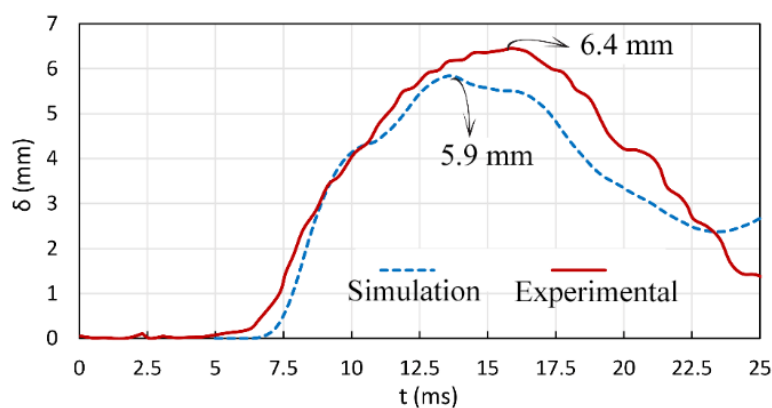


**Fig. 8.** Comparison of effective plastic strain of RC (failure mode); Sample S1616.

We discuss the maximum displacement at the midpoint of the RC beam and the impact force parameters. For the purpose of verifying the numerical model, the bending failure mode of concrete (crack pattern) that occurs after hammer contact is also assessed.

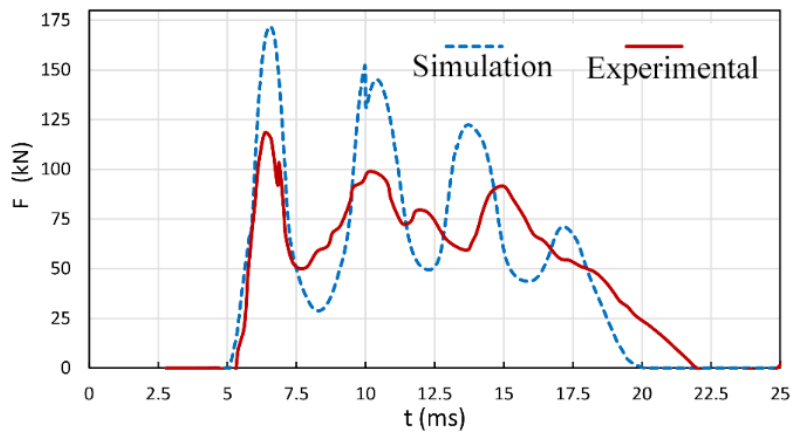
The primary aim of this study is to validate a sample of experimental tests conducted by Fujikake et al. [14]. Once the accuracy of the numerical model has been verified, several parametric analyses can be performed using it. A total of 12 samples of RC beams were assessed for their response to impact [14]. In this study, we have selected the S1616 sample by 0.15 m drop height for precise verification among these samples.

Fig. 8 shows the numerical simulation results with LS-DYNA FE software for the effective plastic strain (bending failure mode) of RC beam sample S1616. As can be seen in the contour of the plastic strain, the bending failure modes are consistent with the results of the drop impact test in Fig. 7 at a height of 0.15 m.



**Fig. 9.** Comparison of mid span displacement for Sample S1616.

Concrete vertical displacement comparison at mid span for the test and the numerical model for sample S1616 with a fall height of 0.15 m is shown in Fig. 9. The trend of the deflection of the RC beam for the numerical model and the test are similar. The maximum value of the displacement of the middle of the concrete beam span is 6.4 mm in the drop impact test and 5.9 mm in the numerical simulation. The difference is less than 0.5 mm (less than 8%), which indicates the good agreement of the obtained results.



**Fig. 10.** Comparison of impact force for test and FE model; Sample S1616.

In Fig. 10, the impact force for the test and the FE model for the S1616 sample with a fall height of 0.15 m are obtained. As can be seen, the impact force starts with a high amplitude and then with a relatively low amplitude, with several consecutive peaks that reach zero in about 20ms. The numerical model's trend of changes and the number of maximum points match the experimental results (Fig. 10). The peak value shows a difference between numerical and experimental models. As can be seen in Fig. 3, the impactor geometry used in the drop hammer test was not exactly hemispherical with a radius of 90 millimeters, compared to the numerical model. This is the reason for the observed discrepancy. In this regard, it is important to point out that we considered the hemisphere shape, which is the closest geometry of the impactor in the experimental setup.

The mesh convergence study is shown in Fig. 11 for the element sizes of 5, 10, and 20 mm, which models have the number of elements 596512, 75902, and 10982, respectively. As can be seen, RC beam mid-span deflection (Fig. 11-a) and the impact force (Fig. 11-b) as well as the change trends of the graphs for three different element sizes, are close to each other. For this reason, in order to save time and cost of numerical calculations, the element size of 10 mm is considered for analysis.

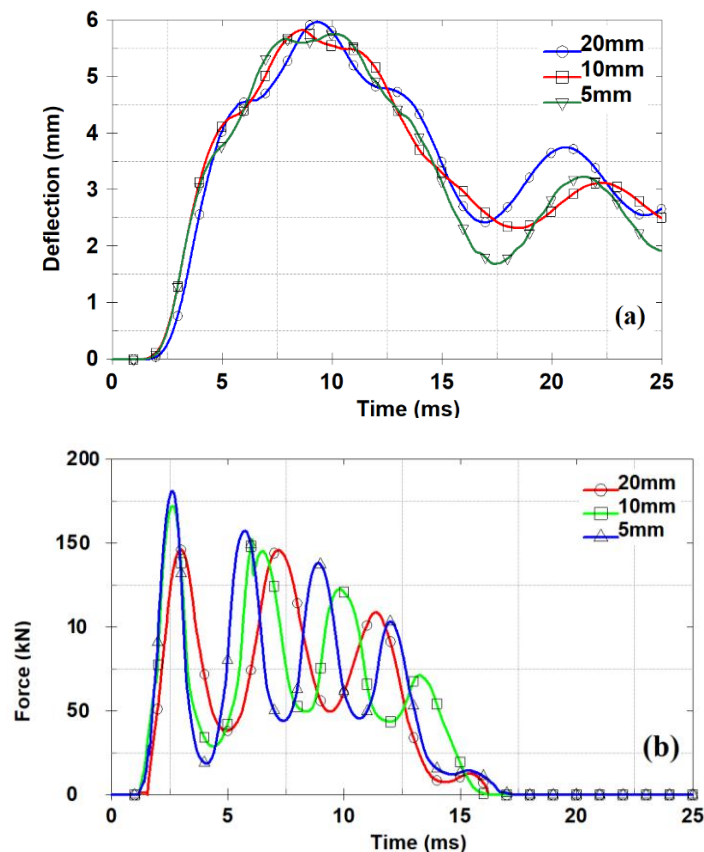


**Fig. 11.** Mesh convergence study; (a) RC beam deflection, (b) Impact force.

#### 4.2. Effect of the loading rate (LR)

By validating the numerical model with experimental data, in this section, the parametric study is performed for the loading rate (LR), in other words, the instantaneous velocity of hammer-RC beam impact. For this purpose, to observe the different behavior of S1616 the loading rates from low to high rates of 2, 4, 6, 8, and 10 m/s are considered. As expected, the deformation of the middle of the RC beam should increase with the increase in the loading rate. Fig. 12 shows that the maximum deflection occurs at LR=10 m/s 10 with 184 mm.

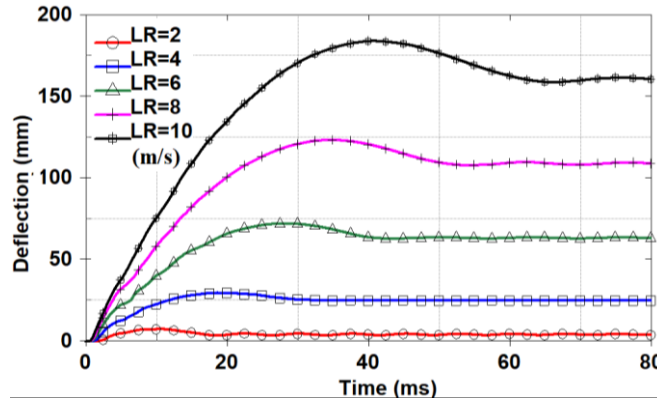


Fig. 12. Deflection at different loading rates.

The maximum impact force under different loading rate conditions is shown in Fig. 13. With the gradual increase of the loading rate from LR=2 m/s to LR=10 m/s, the impact force also increases from 189 kN to 900 kN, respectively.

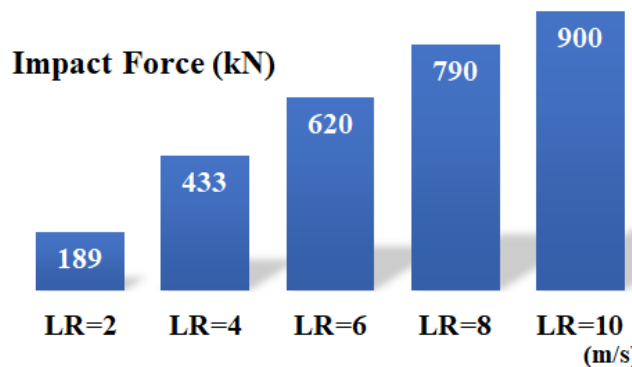


Fig. 13. Maximum impact force at different loading rates.

As expected, the contour of the effective plastic strain of concrete (Fig. 14) shows that the lowest and highest flexural failure modes occur at LR=2 m/s and LR=10 m/s, respectively.

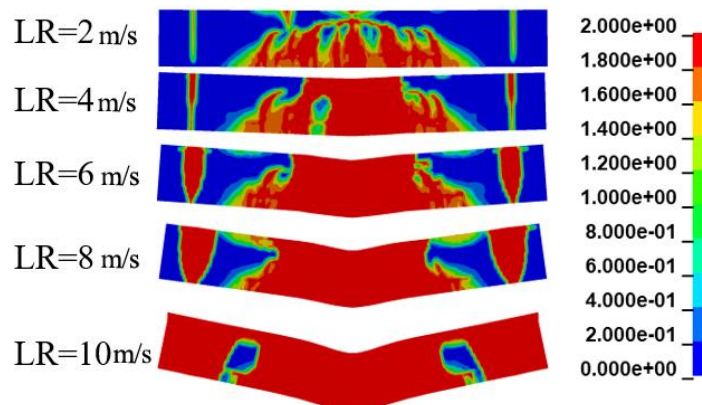


Fig. 14. Concrete plastic strain contour at different loading rates (m/s).



Regarding LR=10 m/s for low (32 MPa) to high (52MPa) compressive strength, impact force is increased by approximately 31%.

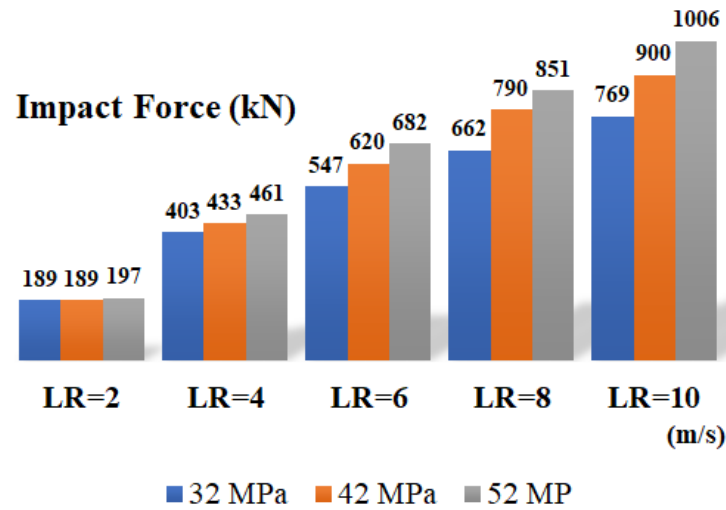


Fig. 16. Impact force at different concrete strengths and loading rates.

## 5. Research significance

In this study, a nonlinear FE numerical model for predicting the bending failure mode of RC beam is developed using LS-DYNA. In 3D analyses, the speed of numerical calculations for this FE code is significantly high compared to other numerical research.. The obtained results are significant for the structural design and evaluation of reinforced concrete columns subjected to impact. We validate the numerical model by comparing it with laboratory data with a reasonable level of accuracy. The material model of the RC beam in this work can describe concrete's complex compression and tension behavior at varied strain rates., as well as predicting the crack pattern of concrete. The proposed FE model enables a comprehensive parametric study for various impact loading analyses, such as the bridge structure under vehicle collisions.

## 6. Conclusion

This work analyzes RC beam bending failure modes under drop hammer impact using experimental and numerical modeling methods. The hammer's free fall impact on RC is simulated using advanced LS-DYNA software and FE numerical approach. The numerical model can predict an accurate response of RC beam bending for failure modes and crack patterns under impact forces. For a wide range of impact loading analyses, including those involving bridge structures and vehicle crashes, the proposed FE model allows for an extensive parametric investigation in future studies.

Deformation in the middle of the beam span and impact load are two important indexes to evaluate the RC beam damage. The results show that the maximum displacement of the concrete at mid span in the test and numerical simulation have less than 8% difference, which indicates a good agreement of the obtained results. The effective plastic strain contour of the RC beam sample S1616 indicates the similarity of the flexural failure modes with the experimental results at the fall height of 0.15 m, and therefore the validity of the numerical model is confirmed.

This model can be used to develop parametric studies including fall height, configurations of longitudinal and transverse rebar, impact load conditions, compressive strengths of concrete, etc. to evaluate the failure modes of RC beams. In this paper, a parametric study was conducted for 5 different loading rates and 3 concrete compressive strengths. The results show that:

1. The mid span displacement is decreased by approximately 10% for every 10 MPa increase in concrete compressive strength (32, 42, and 52 MPa).
2. The concrete's compressive strength at low loading rates (LR = 2 m/s) does not have a major effect on the impact forces.
3. At a low compressive strength of 32 MPa to a high compressive strength of 52 MPa, the impact force increases by approximately 31% when LR is 10 m/s.

Due to cost and computing time, the numerical model for impact cannot accurately model long RC beams or simulate high strain rate impact conditions. To take on these issues, a more efficient numerical model with improved computational precision is needed.

## Notation

$A_s$	Rebar area, mm <sup>2</sup>
$RM$	Bending resistance of rebar, kN
$RS$	Shear resistance of rebar, kN
$D$	Rebar dimension, mm
$a_0, a_1, a_2$	Constant of triaxial compression test
$p$	Confining pressure of concrete at failure level, MPa
$\Delta\sigma_m$	Concrete stress at maximum failure level, MPa
$\Delta\sigma_y$	Concrete stress at yield failure level, MPa
$\Delta\sigma_r$	Concrete stress at residual failure level, MPa
$\Delta\sigma_e$	Concrete stress at advanced failure level, MPa
$r_f$	Enhancement factor for concrete strength
$f_h$	Hardening function
$\varepsilon_{eff}^p$	Effective plastic strain
$\sigma_0$	Initial yield stress, MPa
$E$	Stiffness, MPa
$E_t$	Tangent stiffness, MPa
$\dot{\varepsilon}$	Strain rate
$E_p$	Plastic stiffness
$\rho$	Density, $g/cm^3$
$\beta$	Strain rate parameter
$\nu$	Poisson ratio

## Funding

No outside funding supported this research.

## Conflicts of interest

The authors do not declare any conflicts of interest.

## Authors contribution statement

**A. Rahmati Alaei:** Writing & Editing – main draft, Visualization, Engineering software, Methodology, Numerical analysis, Data management, Conceptualizing.

**M. Khatami:** Offering the initial study idea Writing – review & editing.

## References

- [1] Fang C, Rasmussen JD, Bielenberg RW, Lechtenberg KA, Faller RK, Linzell DG. Experimental and numerical investigation on deflection and behavior of portable construction barrier subjected to vehicle impacts. *Eng Struct* 2021;235:112071. doi:10.1016/j.engstruct.2021.112071.
- [2] Peyman S, Heydari Digesara P. Investigation of crack propagation behavior of impact-resistant functionally graded concrete. *Amirkabir J Civ Eng* 2020;51:1111–28.
- [3] Abadel A, Abbas H, Siddiqui N, Elsanadedy H, Almusallam T, Al-Salloum Y. Numerical investigation of projectile impact behavior of hybrid fiber-reinforced concrete slabs. *Case Stud Constr Mater* 2023;19:e02533. doi:10.1016/j.cscm.2023.e02533.
- [4] Day KW. *Concrete mix design, quality control and specification*. CRC press; 2006.
- [5] Dalvand A, Sivandipour A. Assessment of Statistical Variations in Experimental Impact Resistance and Energy Absorption of High Strength Concrete. *Exp Res Civ Eng* 2015;2:133–41.
- [6] Reddy ARP, Sreenivasappa NM, Prabhakara R, Reddy HNJ. Effect of Steel Ratio on Dynamic Response of HSC Two Way Slab Strengthened by Entrenched CFRP Strips Using Drop Test. *Recent Trends Civ. Eng. Sel. Proc. ICRTICE 2019*, Springer; 2020, p. 157–73.
- [7] Fujikake K, Senga T, Ueda N, Ohno T, Katagiri M. Study on Impact Response of Reactive Powder Concrete Beam and Its Analytical Model. *J Adv Concr Technol* 2006;4:99–108. doi:10.3151/jact.4.99.
- [8] Mollaei S, Babaei M, JalilKhani M. Assessment of damage and residual load capacity of the normal and retrofitted rc columns against the impact loading. *J Rehabil Civ Eng* 2021;9:29–51.
- [9] Bin Cai, Lu S, Fu F. Behavior of steel fiber-reinforced coal gangue concrete beams under impact load. *Eng Struct* 2024;314:118306. doi:10.1016/j.engstruct.2024.118306.
- [10] Zhang Y, Cheng X, Diao M, Li Y, Guan H, Sun H. FRP retrofit for RC frame substructures against progressive collapse: Scheme optimisation and resistance calculation. *Eng Struct* 2023;289:116289. doi:10.1016/j.engstruct.2023.116289.
- [11] Dhiman P, Kumar V. Numerical investigation of reinforced concrete beams under impact loading. *Asian J Civ Eng* 2024;25:537–54. doi:10.1007/s42107-023-00793-0.
- [12] Sun J-M, Chen H, Yi F, Ding Y-B, Zhou Y, He Q-F, et al. Experimental and numerical study on influence of impact mass and velocity on failure mode of RC columns under lateral impact. *Eng Struct* 2024;314:118416. doi:10.1016/j.engstruct.2024.118416.
- [13] Zhou Y, Cheng X, Li Y, Liu F. Simplified numerical model for the collapse analysis of RC frame under oblique impact. *Mag Concr Res* 2023;76:159–75.
- [14] Khomami Abadi M, Alijani A. A new approach to finite element modeling of crack in RC beams. *Concr Res* 2018;11:51–65.
- [15] Anil Ö, Durucan C, Erdem RT, Yorgancilar MA. Experimental and numerical investigation of reinforced concrete beams with variable material properties under impact loading. *Constr Build Mater* 2016;125:94–104. doi:10.1016/j.conbuildmat.2016.08.028.
- [16] Ožbolt J, Sharma A. Numerical simulation of reinforced concrete beams with different shear reinforcements under dynamic impact loads. *Int J Impact Eng* 2011;38:940–50. doi:10.1016/j.ijimpeng.2011.08.003.
- [17] Rezazadeh Eidgahee D, Soleymani A, Jahangir H, Nikpay M, Arora HC, Kumar A. Estimating the load carrying capacity of reinforced concrete beam-column joints via soft computing techniques. *Artif. Intell. Appl. Sustain. Constr.*, 2024. doi:10.1016/B978-0-443-13191-2.00014-6.
- [18] Fakharian P, Nouri Y, Ghanizadeh AR, Safi Jahanshahi F, Naderpour H, Kheyroddin A. Bond strength prediction of externally bonded reinforcement on groove method (EBROG) using MARS-POA. *Compos Struct* 2024;349–350:118532. doi:10.1016/j.compstruct.2024.118532.
- [19] Chen L, Fakharian P, Rezazadeh Eidgahee D, Haji M, Mohammad Alizadeh Arab A, Nouri Y. Axial compressive strength predictive models for recycled aggregate concrete filled circular steel tube columns using ANN, GEP, and MLR. *J Build Eng* 2023;77:107439. doi:10.1016/j.jobbe.2023.107439.
- [20] Aminakbari N, Kabir MZ, Rahai A, Hosseinnia A. Experimental and Numerical Evaluation of GFRP-Reinforced Concrete Beams Under Consecutive Low-Velocity Impact Loading. *Int J Civ Eng* 2024;22:145–56. doi:10.1007/s40999-023-00883-9.

- [21] Nouri Y, Ghanbari MA, Fakharian P. An integrated optimization and ANOVA approach for reinforcing concrete beams with glass fiber polymer. *Decis Anal J* 2024;11:100479. doi:10.1016/j.dajour.2024.100479.
- [22] Jahangir H, Hasani H, Esfahani MR. Wavelet-based damage localization and severity estimation of experimental RC beams subjected to gradual static bending tests. *Structures* 2021;34:3055–69. doi:10.1016/j.istruc.2021.09.059.
- [23] Soleymani A, Jahangir H, Rashidi M, Mojtahedi FF, Bahrami M, Javanmardi A. Damage Identification in Reinforced Concrete Beams Using Wavelet Transform of Modal Excitation Responses. *Buildings* 2023;13:1955. doi:10.3390/buildings13081955.
- [24] Miyagawa T, Morikawa H, Otsuki N, Miyamoto A, Eguchi K, Hamada H, et al. STANDARD SPECIFICATION FOR CONCRETE STRUCTURES,-2001 “MAINTENANCE.” 대한토목학회 학술대회 2003:5629–40.
- [25] Fujikake K, Li B, Soeun S. Impact Response of Reinforced Concrete Beam and Its Analytical Evaluation. *J Struct Eng* 2009;135:938–50. doi:10.1061/(ASCE)ST.1943-541X.0000039.
- [26] Hallquist JO. LS-DYNA keyword user’s manual. Livermore Softw Technol Corp 2007;970:299–800.
- [27] Malvar LJ, Crawford JE, Wesevich JW, Simons D. A plasticity concrete material model for DYNA3D. *Int J Impact Eng* 1997;19:847–73. doi:10.1016/S0734-743X(97)00023-7.
- [28] Kumar P, Srivastava G. Effect of fire on in-plane and out-of-plane behavior of reinforced concrete frames with and without masonry infills. *Constr Build Mater* 2018;167:82–95. doi:10.1016/j.conbuildmat.2018.01.116.
- [29] Nam J-W, Kim H-J, Kim S-B, Yi N-H, Kim J-HJ. Numerical evaluation of the retrofit effectiveness for GFRP retrofitted concrete slab subjected to blast pressure. *Compos Struct* 2010;92:1212–22. doi:10.1016/j.compstruct.2009.10.031.
- [30] Cuong NH, An H, Han T-V, An S, Shin J, Lee K. Structural test and FEM analysis of a thermal bridge connection employing the UHPC system for concrete cladding wall. *Results Eng* 2024;22:102191. doi:10.1016/j.rineng.2024.102191.
- [31] Reifarh C, Castedo R, Santos AP, Chiquito M, López LM, Pérez-Caldentey A, et al. Numerical and experimental study of externally reinforced RC slabs using FRPs subjected to close-in blast loads. *Int J Impact Eng* 2021;156:103939. doi:10.1016/j.ijimpeng.2021.103939.